

Dynamics of photoinduced phonon entanglement generation between remote electron-phonon systems

Kunio Ishida*

*School of Engineering and Center for Optical Research and Education,
Utsunomiya University, Utsunomiya, Tochigi 321-8585, Japan*

Hiroaki Matsueda

*Department of Applied Physics, Graduate School of Engineering,
Tohoku University, Sendai 980-8579, Japan*

Abstract

The generation of phonon entanglement between photoirradiated remote systems is numerically studied. Analysis by the quantum mutual information reveals that laser pulse irradiation induces phonon entanglement with a certain incubation period, which is determined by the creation time of phonons. This behavior is consistent with the motion of composite modes of the system, which are derived from the Heisenberg equation of motion for the amplitude operator of the Stokes light. These results show that the dynamics of the phonon entanglement can be observed by time-resolved spectroscopy.

The recent progress of ultrashort pulse laser technology has made it possible to observe the time evolution of quantum-mechanical states in the coherent regime. As the transient properties of condensed matter have been studied by various time-resolved techniques[1–4], the light control of quantum many-body states has become an intriguing problem, which motivated us to pay attention to the quantum nature of light-matter interaction.

Quantum entanglement is a key concept in quantum information processing. It also gives an insight into various aspects of quantum many-body states[5, 6], e.g., the quantum phase transition[7]. Considering that the injection of optical excitation induces cooperative phenomena of electrons and/or lattices[8–10], the photoinduced quantum phase transition is a next step in the coherent control of condensed matter. Hence, in order to manipulate these phenomena, it is important to reveal the mechanism of cooperative phenomena on excited-state manifolds by means of the quantum information theory. These types of quantum-mechanical control are reminiscent of “quantum materials” realized as transient states of materials under an external field[11], where profound knowledge of quantum many-body states is required to obtain a material design method in the transient regime.

Recently, the generation of quantum entanglement between remote systems has attracted our attention, since nonlocal correlation between qubits plays an essential role in advanced quantum information technologies. Recent experimental studies exemplified methods of light-mediated entanglement generation between non-interacting systems, which showed that ultrashort laser pulses generate entanglement between phonons in diamond crystals[12], and that quantum correlation between distant quantum dots is induced by microwave irradiation[13]. We stress that these studies provide us a clue for understanding the relationship between the quantum entanglement and the dynamical control of many-body states in materials. Therefore, in this study, we numerically investigate the dynamics of quantum entanglement generation in remote systems by light irradiation. Although the manipulation of multi-qubit systems has only been performed at low temperatures[13], an experimental study on phonon entanglement showed that they can be manipulated at room temperature[12], which is advantageous not only for practical applications but also for studying photoinduced structural changes[14] in the coherent regime. Hence, we treat electron-phonon systems as material systems and focus on the dynamics of phonon entanglement generation between remote systems. Furthermore, as shown in previous studies on the Tavis-Cummings model[15] of multi-qubit entanglement[16–18], quantized light is necessary for photoinduced entangle-

ment generation, and thus we should consider a model of electron-phonon-photon systems.

Since the entire system is composed of multiple types of quanta, we must consider multipartite entanglement to study phonon entanglement. Hence, we discuss an appropriate measure for phonon entanglement. Since the concurrence or tangle is only applicable to the evaluation of multi-qubit entanglement[16–18], we instead discuss the quantitative properties of phonon entanglement by two different methods. First, we calculate the quantum mutual information, which is interpreted as the relative entropy of the reduced density matrix for the phonon subspace to its closest separable state[19, 20]. The second method uses a set of composite modes derived from the Heisenberg equation of motion[21, 22]. We studied the mechanism of phonon entanglement generation by comparing the results of the two methods.

The measurement of entanglement properties is also of interest from an experimental viewpoint. Since scattered light carries information on the nonlocal correlation between material systems, we discuss the detection of entanglement by time-resolved spectroscopy. We found that it is possible to access the dynamical properties of entanglement generation by the heterodyne detection of the Stokes light.

We aimed to calculate the quantum dynamics of multiple electron-phonon systems irradiated by photons. For this purpose, we employ a model of M non-interacting electron-phonon systems. When all of the systems interact with multimode photons, the Hamiltonian is described by[23]

$$\begin{aligned} \mathcal{H} = & \sum_{i=1}^3 \Omega_i c_i^\dagger c_i \\ & + \sum_{j=1}^M \left[\omega a_j^\dagger a_j + \sigma_x^j \left\{ \sum_{i=1}^N \mu_i (c_i^\dagger + c_i) + \lambda \right\} \right. \\ & \left. + \hat{n}_j \{ \nu (a_j^\dagger + a_j) + \varepsilon \} \right], \end{aligned} \quad (1)$$

where a_j and c_i denote the annihilation operators of optical phonons in the j -th material system (system j) and the photons of the i -th mode, respectively. σ_ρ^j ($\rho = x, y, z$) describes the Pauli matrix that operates on the electronic states of the j -th material system, $|g\rangle_j$ (ground state) and $|e\rangle_j$ (excited state). $\hat{n}_j = (\sigma_z^j + 1)/2$ is the excited state electronic population of the j -th system.

We take $\hbar = 1$ and the parameter values are $\omega = 1$, $\mu_i = 0.5$ ($i = 1, 2, 3$), and $\varepsilon = 13.5$. We also set the electron-phonon coupling (Huang-Rhys factor) ν to 3.5, a typical value

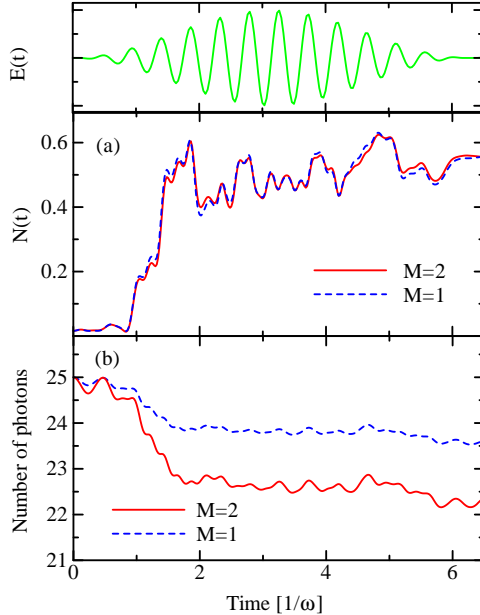


FIG. 1. Top panel: Electric field amplitude of the incident light pulse. (a) Excited-state population $N(t)$ as a function of time. The red line and the blue dashed line correspond to $N(t)$ for $M = 2$ and $M = 1$, respectively. (b) The number photons in the pump mode $\langle c_1^\dagger c_1 \rangle$ for $M = 2$ (red line) and $M = 1$ (blue dashed line).

for various materials[24, 25]. Since Raman scattering is one of the primary processes in the excitation of electron-phonon systems, three photon modes corresponding to the pump mode ($\Omega_1 = 13.5$), Stokes mode ($\Omega_2 = 12.5$), and anti-Stokes mode ($\Omega_3 = 14.5$) are taken into account.

The time-dependent Schrödinger equation for Hamiltonian (1) was numerically solved for $M = 2$ to obtain the wavefunction $|\Phi(t)\rangle$. The initial condition is given by $|\Phi(0)\rangle = |\alpha_1\rangle \otimes |\alpha_2\rangle \otimes |\alpha_3\rangle \otimes |G\rangle_1 \otimes |G\rangle_2$, where $|\alpha_i\rangle$ denotes a coherent state parameterized by α_i for the i -th photon mode and $|G\rangle_j$ is the ground state of the j -th electron-phonon system. In the present study we set $\alpha_1 = 5$ and $\alpha_2 = \alpha_3 = -2.5$ in order to describe a train of optical pulses.

An overview of the dynamics of the system is obtained by monitoring the behavior of observables. We show the excited-state population $N(t) = \langle \hat{n}_1 \rangle \equiv \langle \Phi(t) | \hat{n}_1 | \Phi(t) \rangle$ as a function of time in Fig. 1-(a), for example. The blue dashed line in the figure is $N(t)$ for $M = 1$, and the top panel of the figure shows the expectation value of the electric field amplitude of the incident pulse $E(t)$. The two lines in Fig. 1-(a) almost coincide, as systems

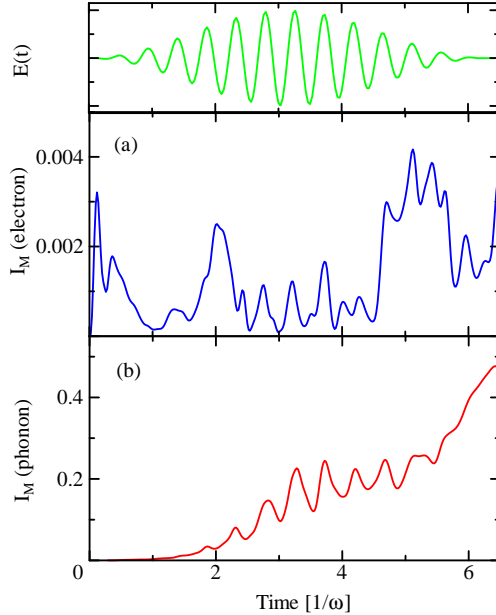


FIG. 2. Top panel: Electric field amplitude of the incident light pulse. Quantum mutual information $I_M(t)$ for (a) $A, B =$ electrons, and (b) $A, B =$ phonons.

1 and 2 do not interact directly. The slight difference between them originates from two factors. One is the difference in the number of absorbed photons. As shown in Fig. 1-(b), it linearly depends on M , and thus the reaction from the photon to the electron is different between the two cases. The other is the quantum correlation between systems 1 and 2, which is mediated by irradiated photons. Obviously, this effect does not exist for $M = 1$, which we focus on in this paper.

It is necessary to choose a measure for entanglement in order to discuss the quantum correlation itself. As we mentioned before, the entanglement between phonons should be referred to as multipartite or mixed-state entanglement[26] in the present case. Among various measures for multipartite entanglement, we calculated the quantum mutual information $I_M(t)$, defined by $I_M(t) = S_A(t) + S_B(t) - S_{A \otimes B}(t)$. S_α denotes the von Neumann entropy of the reduced density matrix ρ_α on the subsystem α [19, 27].

Figures 2-(a) and (b) show $I_M(t)$ as functions of t for electron entanglement ($A, B =$ electrons) and phonon entanglement ($A, B =$ phonons), respectively. First, we found that $I_M(t)$ has finite values under pulse irradiation in both cases. Regarding the electron entanglement, $I_M(t)$ for electrons increases immediately after the photoirradiation starts, while $I_M(t)$ for phonon entanglement remains at a small value for $t < 1$ and starts to increase af-

terwards. These features reflect the different entanglement generation mechanisms between electrons and phonons, which we study by considering the composite modes related to the corresponding quantum correlations.

As we mentioned before, the scattered light carries information on quantum correlations. This means that the measurement of entanglement dynamics is possible by detecting the scattered light, which enables us to discuss the relationship between $I_M(t)$ and physical properties. However, since the signal of the phonon quantum correlation on the scattered light is weak, we consider the heterodyne detection of the output light pulse for which the frequency of the reference light is Ω_1 . Hence, we calculated the signal on the Stokes light, which is proportional to $\sqrt{\Omega_2}\text{Re}(\langle c_2 \rangle e^{i\Omega_1 t})$. Moving on to the Heisenberg picture, $c_2(t)$ satisfies the equation of motion given by

$$i\frac{dc_2(t)}{dt} = [c_2(t), \mathcal{H}] = \Omega_2 c_2(t) + \mu_2 \sum_{j=1}^2 \sigma_x^j(t), \quad (2)$$

where the operators with explicit time dependence are expressed in the Heisenberg representation. The first term of the rhs of Eq. (2) describes the beat of the photons, while the second term represents the effect of the electron-photon (dipole) interaction. Hence, the quantum correlation between systems 1 and 2 is reflected in the Stokes light through $\sigma_x^j(t)$.

However, we note that $\sigma_x^j(t)$ also contains the dynamical properties of individual electron-phonon systems that are irrelevant to the entanglement between the two systems. Therefore, we subtract the corresponding signal for $M = 1$ from that for $M = 2$, and the signal on the Stokes light is described by

$$\Delta I(t) \sim \mu_2 \sqrt{\Omega_2} \text{Im} e^{i\omega t} \sum_{j=1}^2 \int_0^t e^{i\Omega_2 t'} (\langle \sigma_x^j(t') \rangle - \bar{s}_x(t')) dt', \quad (3)$$

where $\bar{s}_x(t)$ denotes the expectation value of $\sigma_x(t)$ for $M = 1$.

The dynamics of $\sigma_x^j(t)$ is also studied using its the equation of motion. The equation of motion does not close in any order, and we obtain a series of composite operators dressed with various types of fluctuations of electrons/phonons/photons in the equations of motion at each order[21, 22, 27]. Hence, the time dependence of $\sigma_x^j(t)$ is determined through the motion of these composite modes, and we focus on those relevant to the quantum correlation between systems 1 and 2 to study the dynamics of $I_M(t)$. After simple calculations[27], we found that the operator relevant to the intersystem quantum correlation first appears in the form of $\sigma_x^1(t)\sigma_z^2(t)$. For phonon entanglement, the corresponding operator is obtained

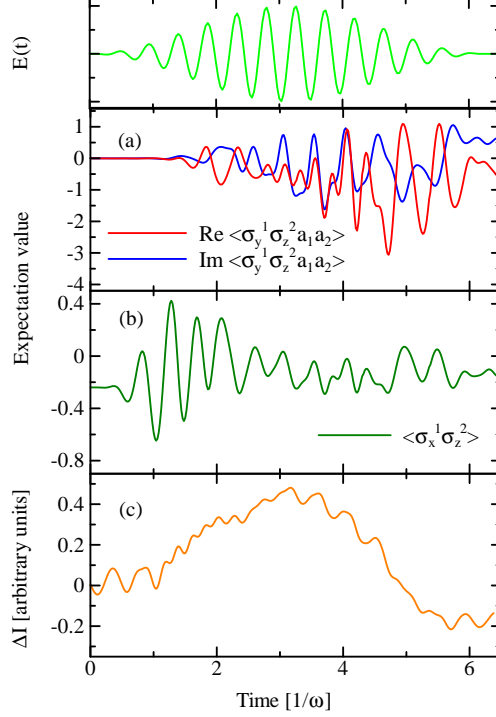


FIG. 3. Top panel: Electric field amplitude of the incident light pulse. Expectation values of the composite operators for (a) $\sigma_x^1(t)\sigma_z^2(t)$ and (b) $\sigma_y^1(t)\sigma_z^2(t)a_1(t)a_2(t)$. (c) Signal of heterodyne detection $\Delta I(t)$. $\langle \sigma_y^1(t)\sigma_z^2(t)a_1(t)a_2(t) \rangle$ is relevant to the time evolution of $\Delta I(t)$ as shown in Ref. [27].

as, for example, $\sigma_y^1(t)\sigma_z^2(t)a_1(t)a_2(t)$. These operators do not appear in the case of a single electron-phonon system ($M = 1$), while the other intrasystem operators do. We also stress that they are obtained only when the quantization of light is taken into account, which reflects the fact that the interaction with the classical electromagnetic field is responsible for the local operations with classical communication (LOCC)[28] in the present configuration.

Figures 3-(a)-(c) respectively show $\langle \sigma_x^1 \sigma_z^2 \rangle$, $\langle \sigma_y^1 \sigma_z^2 a_1 a_2 \rangle$, and $\Delta I(t)$ as functions of time. When the incident light is turned on, the time evolution of the system causes the values of these quantities to change. Regarding the expectation values of the composite operators, $\langle \sigma_x^1 \sigma_z^2 \rangle$ has a finite value even for $t \sim 0$, which contributes to the generation of quantum correlation between electronic states of systems 1 and 2. Accordingly, $I_M(t)$ for electron entanglement rapidly grows as shown in Fig. 2. In contrast, $\langle \sigma_y^1 \sigma_z^2 a_1 a_2 \rangle$, which is relevant to the phonon entanglement, grows with a certain delay (~ 1) since it is proportional to the number of excited phonons. An important feature shown in Figs. 2-(b) and 3-(b) is that

the overall behavior of $\langle \sigma_y^1 \sigma_z^2 a_1 a_2 \rangle$ synchronizes with the growth of $I_M(t)$ at the beginning of photoirradiation, which shows that the growth dynamics of $I_M(t)$ for $t < 2$ can be understood by the motion of the relevant composite mode $\sigma_y^1 \sigma_z^2 a_1 a_2$. In other words, the incubation period in $I_M(t)$ corresponds to the creation time of phonons.

Although $E(t)$ is small for $t < 1$, photons in each mode interact with electrons and there is a slight change of the number of the photons as shown in Fig. 1-(b). As a result, electron entanglement appears when the light irradiation starts. In contrast, as shown in Fig. 1-(a), electronic population transfer does not take place when $E(t)$ is small, and the creation of phonons is suppressed during this period of time. Thus, Fig. 2-(b) shows that phonon entanglement is generated after a certain phonon population has accumulated in the system.

Figure 3-(c) shows that $\Delta I(t)$ increases after weak oscillation for $t < 1$. Since this change of behavior is similar to that in $I_M(t)$ and $\langle \sigma_y^1 \sigma_z^2 a_1 a_2 \rangle$, we conclude that the measurement of $\Delta I(t)$ will give information on phonon entanglement, i.e., the heterodyne detection of the Stokes light is suitable for observing the dynamical properties of phonon entanglement generation.

In this paper, we studied the dynamics of entanglement generation between remote systems by the irradiation of a quantized light pulse. Employing a model of coupled electron-phonon-photon systems, we found that the quantum mutual information for phonons $I_M(t)$ reveals the dynamics of phonon entanglement generation, and that $I_M(t)$ grows with a certain incubation period during photoirradiation. This feature can be understood from the dynamics of composite modes derived from the Heisenberg equation of motion.

Detection methods of entanglement generation dynamics were also studied and we showed that scattered light, e.g., Stokes light, carries information on phonon entanglement. We derived relevant composite modes for the complex amplitude of the Stokes light and found that its heterodyne detection will help us distill the information on phonon correlation, which slowly increases after a certain number of phonons are created.

As shown in a previous study on phonon entanglement between remote diamond crystals[12], the entanglement is generated as a result of measuring on the scattered light, i.e., measurement corresponds to a disentanglement process between photons and phonons. Under the projection hypothesis, this means that the quantum correlation before measurement is also important for finding appropriate methods for entanglement control. In other words, the study of the transient behavior of entanglement generation reveals the projected subspaces

required to realize designed entangled states.

K.I. is grateful to K. G. Nakamura for fruitful discussion. This work was partly supported by the research funding granted by Utsunomiya University President, JSPS KAKENHI Grant Numbers JP18K03456 and JP18K03474, and the Collaborative Research Project of Laboratory for Materials and Structures, Institute of Innovative Research, Tokyo Institute of Technology, Japan. Numerical calculations were performed on the facilities of the Super-computer Center, Institute for Solid State Physics, the University of Tokyo, Japan, and the computer resources offered under the category of General Projects by Research Institute for Information Technology, Kyushu University, Japan.

* ishd_kn@cc.utsunomiya-u.ac.jp

- [1] K. G. Nakamura, *et al.*, Phys. Rev. **B94**, 024303 (2016).
- [2] M. Gallart, *et al.*, Phys. Rev. **B96**, 041303 (2017).
- [3] T. Ghosh, S. Aharon, A. Shpatz, L. Etgar, and S. Ruhman, ACS Nano **12**, 5719 (2018).
- [4] M. Chergui and E. Collet, Chem. Rev. **117**, 11025 (2017).
- [5] L. Amico, R. Fazio, A. Osterloh, and V. Vedral, Rev. Mod. Phys. **80**, 517 (2008).
- [6] L. Mazza, D. Rossini, R. Fazio, and M. Endres, New J. Phys. **17**, 013015 (2015).
- [7] M. Vojta, Rep. Prog. Phys. **66**, 2069 (2003).
- [8] M. Gao, *et al.*, Nature **496**, 343 (2013).
- [9] M. Först, *et al.*, Nat. Mater. **14**, 883 (2015).
- [10] “*Photoinduced Cooperative Phenomena*”, eds. K. Nasu, K. Ishida, and S. Koshihara, Special Issue, Appl. Sci. (2019).
- [11] D. N. Basov, R. D. Averitt, and D. Hsieh, Nature Mater. **16**, 1077 (2017).
- [12] K. C. Lee, *et al.*, Science **334**, 1253 (2011).
- [13] F. Borjans, X. G. Croot, X. Mi, M. J. Gullans, and J. R. Petta, Nature **577**, 195 (2020).
- [14] K. Ishida and K. Nasu, Phys. Rev. Lett. **100**, 116403 (2008).
- [15] M. Tavis and F. W. Cummings, Phys. Rev. **170**, 379 (1968).
- [16] T. E. Tessier, I. H. Deutsch, A. Delgado, and I. Fuentes-Guridi, Phys. Rev. **A68**, 062316 (2003).
- [17] Z. X. Man, Y. J. Xia, and N. B. An, Eur. Phys. J. **D53**, 229 (2009).

- [18] S. Agarwal, S. M. Hashemi Rafsanjani, and J. H. Eberly, Phys. Rev. **A85**, 043815 (2012).
- [19] B. Groisman, S. Popescu, and A. Winter, Phys. Rev. **A72**, 032317 (2005).
- [20] A. Kumar, Phys. Rev. **A96**, 012332 (2017).
- [21] F. Mancini and A. Avella, Adv. Phys. **53**, 537 (2004).
- [22] T. Otaki, Y. Yahagi, and H. Matsueda, J. Phys. Soc. Jpn. **86**. 084709 (2017).
- [23] K. Ishida, Eur. Phys. J. **D73**, 117 (2019).
- [24] A. Hoffmann, B. K. Meyer, and E. Malguth, in “*Zinc Oxide: From Fundamental Properties Towards Novel Applications*”, volume 120, Springer Series in Materials Science, 233 (Springer, Berlin, Heidelberg, 2010).
- [25] R. Valiev, A. Freidzon, and A. Bereznoy, RSC Adv. **4**, 79 (2014).
- [26] C. H. Bennett, D. P. DiVincenzo, J. A. Smolin, and W. K. Wootters, Phys. Rev. **A54**, 3824 (1996).
- [27] See Supplemental Material for details of the calculation of $I_M(t)$ and the composite modes.
- [28] M. A. Nielsen and I. L. Chuang, “*Quantum Computation and Quantum Information*” (Cambridge University Press, Cambridge, 2010).